Geobiology

Geobiology (2014), **12**, 20–33 DOI: 10.1111/gbi.12066

Microbially enhanced dissolution of HgS in an acid mine drainage system in the California Coast Range

A. D. JEW,[1] S. F. BEHRENS,[2] J. J. RYTUBA,[3] A. KAPPLER,[2] A. M. SPORMANN[4] AND G. E. BROWN JR[1,4,5]

[1]*Surface & Aqueous Geochemistry Group, Department of Geological & Environmental Sciences, Stanford University, Stanford, CA, USA*
[2]*Center for Applied Geoscience, Eberhard KarlsUniversity of Tuebingen, Tuebingen, Germany*
[3]*Mineral Resources Program, U.S. Geological Survey, Menlo Park, CA, USA*
[4]*Department of Chemical Engineering, Stanford University, Stanford, CA, USA*
[5]*Department of Photon Science and Stanford Synchrotron Radiation Lightsource, SLAC National Accelerator Laboratory, Menlo Park, CA, USA*

ABSTRACT

Mercury sulfides (cinnabar and metacinnabar) are the main ores of Hg and are relatively stable under oxic conditions (K_{sp} = 10^{-54} and 10^{-52}, respectively). However, until now their stability in the presence of micro-organisms inhabiting acid mine drainage (AMD) systems was unknown. We tested the effects of the AMD microbial community from the inoperative Hg mine at New Idria, CA, present in sediments of an AMD settling pond adjacent to the main waste pile and in a microbial biofilm on the surface of this pond, on the solubility of crystalline HgS. A 16S rRNA gene clone library revealed that the AMD microbial community was dominated by Fe-oxidizing (orders Ferritrophicales and Gallionellas) and S-oxidizing bacteria (*Thiomonas sp.*), with smaller amounts (≤6%) being comprised of the orders Xanthomondales and Rhodospirillales. Though the order Ferritrophicales dominate the 16S rRNA clones (>60%), qPCR results of the microbial community indicate that the *Thiomonas sp.* represents ~55% of the total micro-organisms in the top 1 cm of the AMD microbial community. Although supersaturated with respect to cinnabar and metacinnabar, microcosms inoculated with the AMD microbial community were capable of releasing significantly more Hg into solution compared to inactivated or abiotic controls. Four different Hg-containing materials were tested for bacterially enhanced HgS dissolution: pure cinnabar, pure metacinnabar, mine tailings, and calcine material (processed ore). In the microcosm with metacinnabar, the presence of the AMD microbial community resulted in an increase of dissolved Hg concentrations up to 500 μg L^{-1} during the first 30 days of incubation. In abiotic control microcosms, dissolved Hg concentrations did not increase above 100 ng L^{-1}. When Hg concentrations were below 50 μg L^{-1}, the Fe-oxidizing bacteria in the AMD microbial community were still capable of oxidizing Fe(II) to Fe(III) in the AMD solution, whereas concentrations above 50 μg L^{-1} resulted in inhibition of microbial iron oxidation. Our experiments show that the AMD microbial community contributes to the dissolution of mercury sulfide minerals. These findings have major implications for risk assessment and future management of inoperative Hg mines worldwide.

Received 5 April 2013; accepted 15 October 2013

Corresponding author: A. D. Jew. Tel.: +1 650 723 7513; e-mail: adamjew@stanford.edu

INTRODUCTION

Mercury from mine sites often poses a major environmental risk to ecosystems downstream of the mines. In California, legacy waste from historical mercury mining in the California Coast Range is found at thousands of abandoned mines (Rytuba, 2003). Although elemental Hg is the main ore material at some California mercury mines (e.g., the Socrates Mine, West Mayacamus District, Sonoma, Co.), the majority of mines have both cinnabar and metacinnabar as primary ore minerals (Linn, 1968; Kim *et al.*, 2000, 2004; Rytuba, 2003; Lowry *et al.*, 2004).

Ore processing was done by roasting HgS-containing ore material at ~700 °C (a process known as calcining), which causes HgS to break down to elemental Hg that was then condensed to the liquid form (Linn, 1968). This process was reasonably effective at recovering Hg from the ore, but a significant amount of untransformed HgS was left in the calcined material. The gangue material (tailings) and roasted ore waste (calcine) were dumped in large piles of waste near the mines.

At Earth's surface under oxic, abiotic conditions, cinnabar and metacinnabar are quite stable, with solubility products of 10^{-54} and 10^{-52}, respectively (Faure, 1991; Krauskopf & Bird, 1995). A number of studies have shown that HgS stability is influenced heavily by reduced sulfur species, polysulfides, and thiol-rich organic matter, but these past studies were conducted under anoxic conditions (Paquette & Helz, 1995, 1997; Ravichandran *et al.*, 1998, 1999; Jay *et al.*, 2000; Benoit *et al.*, 2001; Reddy & Aiken, 2001; Drexel *et al.*, 2002; Aiken *et al.*, 2003; Haitzer *et al.*, 2003; Waples *et al.*, 2005). Because HgS is considered stable in oxic systems the stability of HgS in highly oxic AMD systems has so far not been examined.

Mercury, presumably in the form of zero-valent ion pairs, is converted to methylmercury in anoxic sediments as a co-metabolic product of S-reducing and Fe-reducing bacteria (Compeau & Bartha, 1985; Benoit *et al.*, 1999a,b; King *et al.*, 2000; Ullrich *et al.*, 2001; Fleming *et al.*, 2006); however, methylation by micro-organisms in oxic systems is unknown (Fagerstrom & Jernelov, 1971; Hayashi *et al.*, 1977). Both types of bacteria are generally restricted to anoxic habitats, where polysulfide, reduced sulfur species, and thiol-rich organic matter are generally considered to play a more dominant role in HgS dissolution than micro-organisms due to the strong binding constants and high abundance of abiotic functional groups in anoxic environments.

A number of studies of the effect of Hg-resistant bacteria on the stability of different Hg species have been carried out, but only a few have focused on HgS (Baldi & Olson, 1987; Baldi *et al.*, 1989, 1991; Kalyaeva *et al.*, 2001; Mindlin *et al.*, 2001; Barkay *et al.*, 2003). Baldi and Olson looked at the effect of adding cinnabar to pyrite in the presence of a Hg-resistant strain of *Thiobacillus ferrooxidans*; this study is one of the few that investigated the interaction of HgS with bacteria (Baldi & Olson, 1987). However, that study did not show any bacterially induced dissolution of HgS when cinnabar was the sole mineral substrate. Wiatrowski *et al.* showed that magnetite can convert Hg(II) to Hg(0) (Wiatrowski *et al.*, 2009). Because of the potential impact of Fe-cycling on Hg speciation shown by Wiatrowski *et al.* and the fact that Baldi and Olson found no evidence for Hg-release into solution from HgS alone, it is possible that Hg-release in systems containing FeS_2 and HgS is due more to abiotic Fe redox-cycling than direct microbial activity. However, no mechanisms have been proposed for this release (Wiatrowski *et al.*, 2009). The focus of this study is to show for the first time the direct impact micro-organisms have on the dissolution of relatively stable HgS minerals in oxic mine settings where HgS is considered to be stable.

MATERIAL AND METHODS

Field sampling

Samples were taken from the New Idria AMD settling pond on Aug. 13, 2008. Water and sediment samples were collected in sterile 50 mL polypropylene tubes and immediately stored on ice. The New Idria bacterial consortium used in this work is present as both a biofilm on the surface of the pond and the surface of the pond sediments, genetic analysis of both groups found identical community composition. Inflow water to the settling pond (pH 3.25) was used in the microcosm experiments to best approximate the AMD settling pond environment. The water was filter-sterilized in the field using 0.1 μm Anatop Plus® filters (Whatman Inc.) into acid-cleaned Pyrex bottles. Numerous water samples from the same location were taken for analysis of total carbon, sulfide, Fe(II), total metals, and total Hg content. All water samples, except those collected for total carbon analysis, were filtered using 0.02 μm Anatop Plus® filters into ultra-trace clean, clear borosilicate vials with Teflon® lined lids. Cleaning of glassware for ultra-clean use involved a three step process: (1) detergent bath, (2) 1N HCl acid bath, and (3) 10% BrCl (vials were inverted to have BrCl covering the Teflon® lined lids). Vials were left in each cleaning agent overnight. Between each step, vials and lids were triple rinsed with DDI water and dried in an oven that has never contained Hg-bearing materials at 120 °C. Samples taken for total carbon analysis were filtered using 0.2 μm polyethersulfone filters (Whatman Inc.) into ultra-trace metal clean amber borosilicate vials. Total Hg concentration samples were preserved using 0.5% bromine monochloride following EPA method 1631 (U.S. EPA, 2002). Samples taken for total metal and major anion concentrations were preserved with 2 mL of Ultrex® brand 1N HNO_3 and sent to the United States Geological Survey in Boulder, CO for analysis.

Clone library construction and sequencing

The 16S rRNA gene library was constructed using the top 2 cm of the AMD settling pond sediment. DNA was extracted as described previously following a modified protocol from Zhou *et al.* (Zhou *et al.*, 1996; Behrens *et al.*, 2008). Domain-specific primers were used to amplify almost-full length 16S rRNA genes from the extracted

chromosomal DNA by PCR; for Bacteria, primers GM3F (*Escherichia coli* 16S rRNA position 0008) (Muyzer *et al.*, 1993) and Uni1392R (Lane *et al.*, 1985) were used, and for Archaea, primers 20f (DeLong, 1992) and Uni1392R or 20f and Arch958R (Massana *et al.*, 1997) were used. PCR's were performed as follows: Amplifications were carried out in 50-μL volumes containing a final concentration of 0.5 μM of each primer, 200 μM of each deoxynucleoside triphosphate, 0.5 U of Taq polymerase (Qiagen GmbH, Germany), 200 μg bovine serum albumin (Sigma-Aldrich, St. Louis, MO, USA), and 1 × Qiagen PCR buffer containing 1.5 mM $MgCl_2$ (pH 8.0). One-microliter amounts of the undiluted and 1:10-, 1:100-, and 1:1000-diluted environmental DNA were used as templates. The PCR amplification parameters included an initial denaturation at 94 °C for 5 min, followed by 25 cycles of 94 °C for 1 min, 48 °C for 1 min using the bacteria domain-specific primers, and 58 °C for 1 min using the Archaea domain-specific primers, followed by an elongation step at 72 °C for 1 min. The last cycle was followed by a final extension step at 72 °C for 9 min. PCR amplifications were performed in a PTC-200 gradient cycler (MJ Research, Inc., Watertown, MA, USA). No PCR amplicons were obtained with both Archaea primer combinations. The bacterial PCR products were purified using a QIAquick PCR purification kit (Qiagen GmbH) and ligated into the pCR4 TOPO vector (Invitrogen, Carlsbad, CA, USA). *E. coli* XL10-Gold ultracompetent cells (Stratagene, La Jolla, CA, USA) were transformed with the plasmids following the manufacturer's recommendations. Sequencing was performed by MCLab (South San Francisco, CA, USA) using Taq cycle sequencing with a model ABI 3730XL sequencer (Applied Biosystems). Sequence assembly was done with the program DNA Baser. The presence of chimeric sequences in the clone libraries was determined with the programs Bellerophon and Mallard version 1.02 (Huber *et al.*, 2004; Ashelford *et al.*, 2006). Potential chimeras were eliminated before phylogenetic analysis. Sequence data were analyzed with BLAST and the ARB software package using the SILVA 103 database (release date, 6 June 2010) (Ludwig *et al.*, 2004; Pruesse *et al.*, 2007).

Real-time quantitative PCR

Due to the presence of a single S-oxidizing microbe in the clone library (*Thiomonas sp.*), real-time qPCR analysis of the S-oxidizing microbe was done. Quantification of 16S rRNA genes in the sediment from the AMD settling pond was performed using iQ Sybr Green Supermix (Bio-Rad Laboratories, Hercules, CA, USA), *Thiomonas*-specific primers, and domain-specific primers for Bacteria (see Table 1). Each sample mixture had a 30-μL reaction volume containing 1 × iQ Sybr Green Supermix, forward and reverse primers at a concentration of 500 nM, and 2 μL of the prepared DNA. PCR amplification and detection were conducted in an iQ5 Cycler (Bio-Rad Laboratories). Real-time PCR conditions were as follows: 3 min at 95 °C followed by 40 cycles of 10 s at 95 °C and 45 s at 61.5 °C. As real-time PCR standard dilutions of a plasmid (pCR4 TOPO vector; Invitrogen, Carlsbad, CA, USA) containing a *Thiomonas* sp. 16S rRNA gene from the clone library was used. Real-time PCR data were analyzed using the IQ5 Optical System Software (Version 2.1; Bio-Rad Laboratories). Because the closest sequenced relative of the isolated *Thiomonas* strain from the AMD microbial community is *Thiomonas intermedia* K12, whose genome contains only one 16S rRNA gene operon, the quantified 16S rRNA gene copy numbers obtained with the *Thiomonas* primers were not divided by a specified value to account for multiple rRNA gene operons. Total Bacteria 16S rRNA gene copy numbers were divided by a factor of 4.07 as the average number of rRNA gene operons of the domain Bacteria documented by the ribosomal RNA database (Lee *et al.*, 2009).

HgS dissolution experiment

Sample preparation

Mercury sulfide dissolution experiments were carried out in 250-mL Erlenmeyer flasks that were acid washed in 1N trace-metal grade HCl and then heated at 500 °C to remove any residual Hg on the glass and to sterilize the flasks. Growth media for all microcosms consisted of water from the New Idria AMD system (pH 3.25) that was filter-sterilized in the field with 0.1 μm Anatop Plus® filters (Whatman Inc.) and then re-sterilized in the laboratory with 0.1 μm Anatop Plus® filters under proper sterile laboratory conditions. Four different types of HgS-containing materials were selected for study: cinnabar, metacinnabar, tailings, and calcine. Tailings and calcine material were collected from the New Idria site adjacent to the AMD system, and cinnabar and metacinnabar samples were

Table 1 Real-time PCR primers used in this study

Name	Sequence (5′->3′)	Target group	Annealing Temp	Fragment length (bp)	Reference
Thio636F	GGATGACTATCCGACTGG	*Thiomonas* sp.	55 °C	218	This study
Thio836R	TACTGAACAGTTGCCCGT	*Thiomonas* sp.			This study
Bact341F	CCTACGGGAGGCAGCAG	Bacteria	60 °C	194	Muyzer *et al.* (1993)
Bact534R	ATTACCGCGGCTGCTGGC	Bacteria			Muyzer *et al.* (1993)

purchased from Alfa Aesar with a purity of >99.99%. Tailings and calcine material were dried in a dessicator and then sieved in stainless-steel sieves to a particle size of 89–124 μm. Bulk mineralogy was determined by x-ray diffraction (XRD). Samples were analyzed on a Rigaku Model CM2029 powder x-ray diffractometer using a Cu K_α x-ray source over the 2θ range 5°–70°. Analysis of the resulting diffractograms was done using the Jade X-ray Diffraction Software package (Materials Data Inc., 2002). Identification of minerals present was done by peak matching the four peaks with the highest intensity for each phase. Bulk mineralogy of the tailings material detected by XRD consists of quartz, feldspar, and jarosite. The mineralogy of the calcine waste material consists of quartz, alunite-jarosite, hematite, illite, and feldspar. Though it is known that the tailings material contains iron sulfide minerals (both marcasite and pyrite), the concentrations of these phases are too low for detection with XRD (Linn, 1968). Both the tailings and calcine material contain Hg-bearing phases (predominantly HgS) at concentrations below those detectable by XRD (420 ppm and 690 ppm Hg, respectively). Due to the softness of the HgS crystals, particle size could not be controlled because any manipulation of the HgS powder, such as crushing in a mortar and pestle, resulted in an uncontrollable change in particle size. The solids (cinnabar, metacinnabar, tailings, and calcine) as well as half of the biological samples from the AMD system were sterilized with a ^{137}Cs gamma irradiation source at the Stanford School of Medicine at an exposure rate of 2602 R min^{-1} for 18 h. Sterilization by gamma irradiation was chosen so that cell lysing could be kept to a minimum. Because of the high metal content of the AMD system, autoclaving samples was not done because of the possibility of significant thermodynamic changes to the system resulting in conditions in the microcosms being different from the conditions of the AMD environment.

All microcosms consisted of either 150 mL of AMD water (oxic microcosms, pH = 3.25) or 100 mL of AMD water (anoxic microcosms and abiotic controls, pH = 3.25), and 2 g of mineral substrate; non-abiotic controls were inoculated with 100 μL of either living or killed biofilm material (total protein added to reactors was 7.88 and 8.12 μg, respectively). In total, five different microcosms contained 2 g of one of the four different solids used in these experiments (tailings, calcine, cinnabar, and metacinnabar) and one containing only filtered water as a control. This resulted in a total of 25 microcosm experiments. Of the five different microcosms constructed for each of the different solids used, two were inoculated with living biofilm material (one incubated in an oxic environment and one in an anoxic environment), two were inoculated with gamma irradiated biofilm material (one incubated in an oxic environment and one in an anoxic environment), and one microcosm in which no biofilm material was added. General solution compositions for all microcosms are listed in Table 2, whereas the organics including total and non-purgeable organic carbon are discussed in the Results section. All microcosms were incubated at ambient temperature (21 °C) without agitation to mimic the AMD settling pond conditions. Anoxic microcosms were constructed outside of an anoxic glove box and then immediately placed in the glove box. Anoxic microcosms were removed from the glove box to be sampled under sterile conditions and then were immediately returned to the glove box. This procedure was used for two important reasons: (i) rubber stoppers commonly used in anoxic work will adsorb large amounts of Hg from microcosms, and (ii) sterile conditions using a flame are not possible in an anoxic glove box. Because oxygen diffusion into solution is fairly slow, the increase of oxygen in abiotic microcosms should be minimal. However, the AMD water was not purged of oxygen before the experiment, resulting in some residual oxygen being left in the system for the first 3 days of the experiment run. Though the oxidation of sulfur in both the iron- and mercury sulfides does produce sulfuric acid, the extent of sulfuric acid production for these microcosms is so small that there was no detectable change to the pH of the system, and the pH stayed constant at 3.25 throughout each experiment.

Microcosm sampling and sample preservation

Sampling of the microcosms occurred every 3 days with samples taken for non-purgeable organic carbon (NPOC, 5 mL), total carbon (TC, 4 mL), total Hg (4 mL), sulfide (3 mL), and iron (Fe^{2+} and total Fe, 1 mL). Samples of the oxic microcosms were taken over a total of 30 days, whereas anoxic microcosms were followed for a total of 18 days. NPOC and TC samples were filtered through 0.2 μm polyethersulfone (PES) filters into amber vials and

Table 2 Selected metals and anions in the New Idria AMD water used in the HgS dissolution experiment, August 2008

Analyte	Concentration (mg L^{-1})
Al	88.6
Ca	222
Fe	368
K	45.4
Mg	233
Na	364
Zn	1.8
Mn	3.8
Silica	19.3
Cl	211
F	4
NO3	<0.08
SO4	4587
PO_4	<0.01

stored at 5 °C until analysis. Mercury, sulfide, and iron samples were filtered with 0.02 μm Anatop Plus® filters (Whatman Inc.) to minimize colloidal HgS uptake. Numerous experiments done in the lab using the Anatop Plus® filters (Whatman Inc.) showed no retention or carryover of Hg, sulfide, and Fe. Mercury samples were filtered into clear borosilicate vials with Teflon® lined lids and preserved with 1.5% BrCl. Sulfide samples were filtered into amber borosilicate vials containing 100 μL of 10N NaOH to raise the pH of the solution from 3.25 to 10.0, resulting in the trapping of sulfide as HS^- as well as causing metals to precipitate from solution. Iron samples were filtered into amber borosilicate vials and analyzed for Fe^{2+} and Fe_{Tot}.

Sample analysis

Background concentrations for total metals were analyzed by inductively coupled plasma atomic emission spectrometry (ICP-AES) using a Perkin Elmer Optima 3300 dual view analyzer and inductively coupled plasma mass spectrometry (ICP-MS) using a Perkin Elmer Sciex Elan 6000 analyzer. Background nitrate, chloride, fluoride, and sulfate were measured by ion chromatography (IC) using a Dionex DX-100 Ion Chromatograph. The concentration of protein within the biofilm material added to microcosms was determined using a BioRad® fluorimetric protein assay kit. Iron (II) and Fe_{Tot} concentrations were determined by ferrozine analysis using a Hewlett-Packard model 8452A UV/Vis spectrophotometer with a lower detection limit of 0.5 mg L^{-1} (Stookey, 1970). Total carbon and nonpurgeable organic carbon concentrations were determined using a Shimadzu model TOC-5000A TC/NPOC analyzer with a lower detection limit of 0.1 mg L^{-1}. During analysis, we found that the high metal concentrations contained in the AMD water resulted in passivation of the catalyst in the TC/NPOC analyzer after 4–5 samples. To address this issue, 10 μL of 10N NaOH were added to the samples to precipitate the metals in solution. The samples were then centrifuged at 9300 g for 5 min to settle out the metal precipitate. The supernatant was then taken and 10 μL of 10N HNO_3 was added to drop the sample pH to <4 for NPOC analysis. Several samples were run with and without metal stripping to determine if a significant amount of carbon was being removed from solution as the metal precipitated. The results of the simultaneous sample runs showed less than 1% variation in carbon between samples where the metals were removed vs. those where metal was left in solution. Total carbon within the tailings and calcine material was measured using a Carlo-Erba model NA 1500 C, N, and S analyzer. Sulfide samples were analyzed within 1 h of sampling following the Cline's method for sulfide analysis with a lower detection limit of 0.03 μM (Cline, 1969). Mercury concentrations were measured on a Tekran® 2600 cold vapor atomic fluorescence spectrometer (CVAFS) following EPA method 1631 with a lower detection limit of 0.05 ng L^{-1} (U.S. EPA, 2002).

Hg impact on Fe-oxidation

Water and biofilm sampling was done on February 10, 2010, with sampling methodology the same as described above for the HgS dissolution experiment, solution pH = 4.0. Because this experiment was designed to determine the inhibition effects of Hg on Fe-oxidizing microorganisms, killed controls were not done. Microcosms contained filter-sterilized AMD water with Hg added to determine Hg toxicity to the Fe-oxidizing portion of the community. No Hg-containing solids were added to the microcosms. By not adding Hg-containing solids, only Fe (II) oxidation in solution is assessed, and the Hg concentrations of the microcosms are controlled only by the amount of Hg added and not impacted by the solids. The background Hg concentration for the experiment was 15.7 ± 0.4 ng L^{-1}, which is much lower than the background levels of 100–400 ng L^{-1} measured during the summer months. Mercury was added to the microcosms in the form of $Hg(NO_3)_2$ at the following concentrations: abiotic control, no Hg added (ran in duplicate), 500, 1000, 5000, 10 000, 50 000, and 100 000 ng L^{-1}. The experiment was sampled every 2 days for a total of 18 days. Samples were filtered through 0.02 μm Anatop plus filters and analyzed following the ferrozine protocol on a Hewlett-Packard 8452A UV/Vis spectrophotometer. Samples were analyzed within 1 h of sampling and triplicates of samples showed error to be <0.1%.

Nucleotide sequence accession numbers

The 16S rRNA gene sequences from the clone library have been submitted to EMBL and assigned the following accession numbers: HE587052 to HE587299.

RESULTS

AMD solution chemistry

Total metal concentrations in the New Idria AMD system are typical of other AMD systems (Table 2). Because Fe (II) is one of the dominant metal ions in solution, it is assumed that Fe(II) oxidation is one prominent driver of microbial metabolism in this ecosystem. ICP analyses carried out over several years (data not shown) show that the concentrations of metals in solution are dependent on the amount of rainfall during the winter rainy season, which can cause concentrations to vary threefold. Dry winters result in an increase in metal concentrations during the following summers due to evaporation, whereas wet winters

tend to dilute the metals when the water discharge from underground mine workings increases. The areal extent and thickness of the AMD biofilm vary inversely with metal concentration. Mercury concentrations within the AMD waters are quite low (100 ± 5.2 ng L^{-1}) and vary inversely with the concentrations of other metals in solution between seasons. The dominant anion in solution is sulfate, which is produced by the oxidative dissolution of sulfide-bearing minerals at the site.

16S rRNA GENE CLONE LIBRARY

The 16S rRNA gene clone library of the top 2 cm of the AMD settling pond sediment revealed that the community was dominated by Fe-oxidizing bacteria of the order Ferritrophicales. Clones affiliated with this order comprised more than 60% of the 248 bacterial clones that were obtained (Fig. 1). The second largest group detected in the 16S rRNA gene clone library comprised relatives of the sulfur-oxidizing bacterial genus *Thiomonas* (about 14% of all clones in the library). A member of this bacterial taxa has also been successfully isolated from this field site. In contrast with the 16S rRNA clone library, quantitative PCR analysis with *Thiomonas*-specific primers revealed a relative abundance of this group of sulfur-oxidizing bacteria of about 55% of all bacteria in the top 1 cm of the AMD pond sediment. The total bacterial 16S rRNA gene numbers were $1 \times 10^8 \pm 2 \times 10^7$ copies per g (wet sediment) in this layer. Other bacterial groups also found with relatively high sequence abundance in the 16S rRNA gene clone library were affiliated with the bacterial orders Gallionellales (7% of all clones in the library), Xanthomonadales (6%), and Rhodospirillales (4%). Altogether, the total AMD microbial community was dominated by bacterial taxa known to contain mostly iron-oxidizing, sulfur-oxidizing, as well as acidophilic chemoorganoheterotropic bacteria.

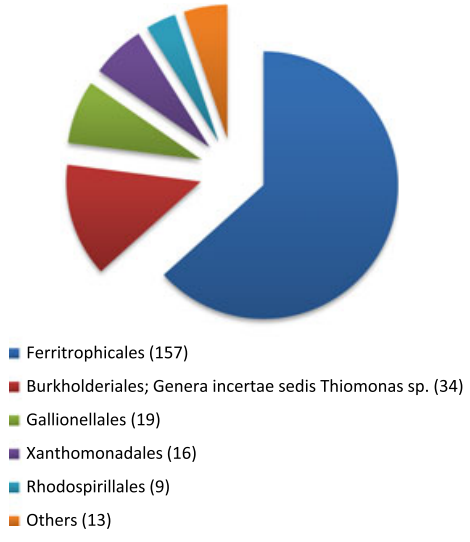

Fig. 1 Summary of the bacterial 16S rRNA gene clone library results of the AMD pond water. Classification was based on the Greengenes classifier using the NCBI taxonomy. Taxonomic orders shown in the pie chart had more than 3% sequence abundance in the clone library. All other obtained sequences are grouped as 'others'. The total number of nearly full length (>1300 bp) 16S rRNA gene clones obtained was 248.

Bacterial dissolution of HgS

Hg concentrations

The background Hg concentration of the New Idria AMD water used in the experiments was 100.8 ± 5.2 ng L^{-1}. Oxic microcosms of living biofilm cells resulted in a significant release of Hg from all four HgS-containing materials (cinnabar, metacinnabar, tailings, and calcine), with Hg concentrations rising from 100.8 ± 5.2 ng L^{-1} to as high as 516.5 ± 23.8 μg L^{-1} over the course of 30 days (Fig. 2). More Hg was released from the calcine material than metacinnabar during the course of the experiments. Extended x-ray absorption fine structure (EXAFS) spectroscopic analysis of the New Idria calcine material showed the presence of eglestonite and montroydite, in addition to HgS polymorphs, within the calcine material (Kim *et al.*, 2000, 2004; Lowry *et al.*, 2004). Because Hg-chlorides and oxides are much more soluble than Hg-sulfides, the higher Hg concentration detected in the calcine microcosm experiment vs. the experiment with metacinnabar is most likely due to more soluble Hg phases in the calcine material, including nanoparticles of HgS (Lowry *et al.*, 2004). EXAFS analysis of the tailings material showed a mixture of cinnabar and metacinnabar (29% and 61% of the Hg speciation, respectively) with 10% HgO (montroydite). The high proportion of metacinnabar and the presence of montroydite are consistent with the tailings material releasing more Hg than cinnabar or metacinnabar. At day 18, Hg concentrations began to level off in the cinnabar and tailings oxic living microcosms, but they continued to increase within the calcine and metacinnabar reactors. Gamma-sterilized AMD water samples incubated aerobically also released Hg from the mineral matrix, but total Hg concentrations were significantly lower than in the biologically active microcosms (Fig. 2). Hg concentrations in abiotic controls started at background levels and dropped to below detection limit (Detection limit was 0.05 ng L^{-1} for Hg in solution) within the first 9 days of incubation suggesting Hg was adsorbing to the mineral matrix (data not shown). Hg-release in the inactivated controls (killed) mirrored the living aerobic microcosms, but the total Hg concentrations were much lower (Fig. 2). Anoxic microcosms of living cells had an initial release of Hg at the start of the experiment, which was assumed to be caused by residual oxygen left in the microcosms. In anoxic micro-

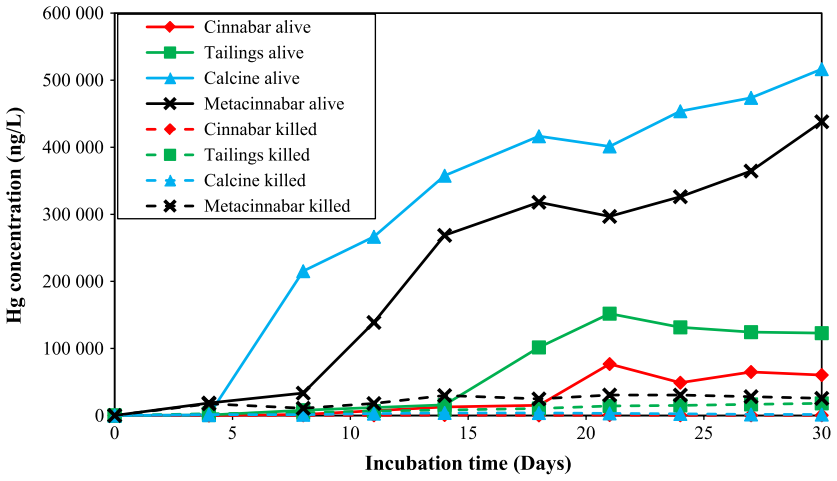

Fig. 2 Mercury release from HgS-bearing materials for oxic microcosms using the New Idria microbial community. Solid lines denote biologically active AMD microbial community material added (7.88 μg of protein added), while dashed lines denote gamma irradiated cells added (8.12 μg of protein added). Error bars are smaller than symbols, error is ± 8% (n = 3). Experiment conducted during August, 2008.

cosms, Hg concentrations are several orders of magnitude below those in the oxic microcosms. After the initial release of Hg, Hg concentrations either leveled off or dropped to levels below detection (Fig. 3). All anoxic microcosms had Hg concentrations below 1.1 ppb, which is significantly lower than that of most of the microcosms incubated under oxic conditions. These results show that oxygen is necessary as the electron acceptor in the dissolution of HgS in the presence of the bacterial consortium.

Sulfide concentrations

Sulfide was detectable at the time of sampling but was not detectable in water collected from the site after 2 days. The background sulfide concentration at the AMD settling pond was 0.8 μM, which was significantly lower than in the preliminary experiments discussed above (up to 45 μM). Sulfide concentrations in previous experiments were measurable for up to a week in microcosms due to high levels of Zn in solution, which stabilized the sulfide as $ZnS_{(aq)}$, as predicted by The Geochemist's Workbench® and Visual Minteq® (Bethke, 2002; Gustafsson, 2009). When approaching the main adit of the New Idria mine, H_2S gas is commonly smelled and emanates from the water exiting the underground mine. The $H_2S_{(g)}$ is usually noticeable up to 100 m from the entrance, but at the time of sampling, the odor was barely noticeable at the adit entrance, suggesting a drop in $H_2S_{(g)}$ production from the underground mine workings.

Total and non-purgeable organic carbon

The New Idria AMD system has a pH ranging between 2 and 5.5 annually, depending on season and rainfall levels. Because of this low pH, the total carbon and non-purgeable organic carbon (NPOC) concentrations are the same. The initial concentration of the NPOC was 2.5 mg L^{-1}. The concentration of all microcosms stayed between 1.2 and 3.5 mg L^{-1}, with no clear trends (data not shown). Ion chromatography (IC) analysis conducted on the AMD

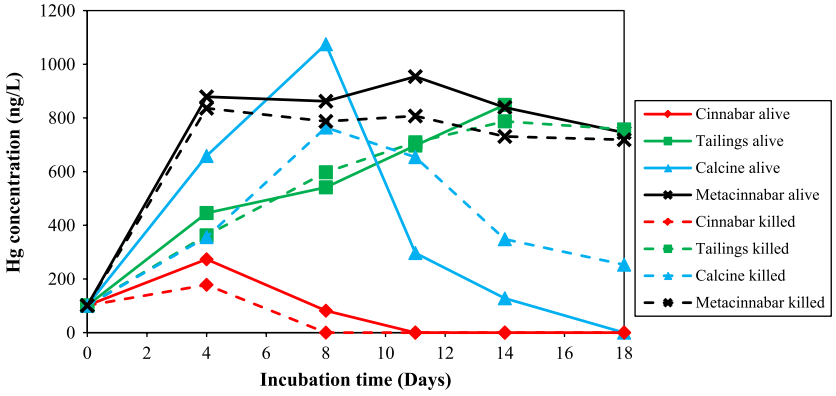

Fig. 3 Mercury release from HgS-containing materials in anoxic microcosms using the New Idria microbial community material. Solid lines denote biologically active microbial community material added (7.88 μg of protein added), whereas dashed lines denote gamma irradiated cells added (8.12 μg of protein added). The initial pulse of Hg in the experiment is due to the growth media not being purged of O_2 prior to beginning of experiment. Error bars are smaller than the symbols, and estimated standard errors are ± 8% (n = 3). The experiment was conducted in August, 2008.

water showed no detectable organic species present with an elution time >30 min. This finding suggests that carbon within the AMD system is in the form of high molecular weight biomolecules, stemming from lyzed microbial cells that have difficulty moving through the IC column. AMD water was also analyzed with UV/VIS spectroscopy to determine if humic and fulvic acids are present in the water. The lack of enhanced absorbance in the UV/VIS spectrum specific for humic and fulvic acids, as outlined by Weishaar *et al.*, suggests that humic and fulvic material are not large contributors to the carbon in the AMD system (Weishaar *et al.*, 2003). The use of the BioRad® protein quantification assay revealed that protein accounted for approximately 60% of the total carbon in the AMD water used as the microcosm medium, suggesting that cellular biomass is the main source of carbon in the ecosystem.

Iron oxidation

The background Fe concentration (369.4 ± 0.4 mg L^{-1}) of the water entering the New Idria AMD settling pond is typical of AMD systems. The total Fe concentration was measured with ICP-OES and Ferrozine, both resulting in values within 1% of each other. The oxidation state of the Fe entering the pond is 100% Fe(II) as determined by Ferrozine. In the oxic living microcosms, the Fe(II) was all oxidized to Fe(III) within 18 days for reactors containing cinnabar, tailings, and calcine material (Fig. 4). All other microcosms in the experiment behaved like the metacinnabar-only microcosm, with an initial drop in Fe(II), which also corresponds to Fe_{tot} concentrations, and then a leveling off of Fe(II) for the remainder of the experiment (Fig. 4). The initial drop in Fe(II) is considered caused by adsorption of Fe to either the solids or the glass wall of the flask as Fe(II) still comprises 100% of the total Fe detected in the microcosms. In the tailings and calcine microcosms containing living cells, the mineral substrate turned yellow during the experiment, indicating that the pyrite and/or marcasite present was oxidized by the biofilm material and precipitated as an Fe(III)-bearing phase (Jarosite). Because of the significant difference in Fe redox behavior between the reactors containing metacinnabar vs. the other three mineral substrates, an additional set of experiments was carried out that examined the effects of Hg solution concentration on Fe-oxidation.

Effects of Hg on iron oxidation

The background Fe_{Tot} concentration for this experiment was 181.3 ± 0.1 mg L^{-1}. Similar to the previous experiments, 100% of the Fe was in the form of Fe(II). Fe(II) oxidized to Fe(III) in 14 days of incubation in all microcosms but the abiotic control and the 100 000 ng L^{-1} of Hg microcosm (Fig. 5). Although an exact Hg concentration required to completely inhibit Fe-oxidation in the microcosms was not established, the Hg concentration required is between 50 000 ng L^{-1} and 100 000 ng L^{-1} for New Idria AMD biofilm. As expected, as Hg concentration increases, the rate of Fe(II) oxidation is retarded (Fig. 5). The inhibition concentration for the Fe-oxidizing bacteria in the New Idria AMD biofilm is much lower than the tolerance of the S-oxidizing bacterium (20 mg L^{-1} Hg) isolated from the site.

DISCUSSION

Clone library, qPCR, and Carbon cycling

The microbial biofilm, both the pond surface and sediment surface communities, in the New Idria AMD system is dominated by two different metabolic types of bacteria: Fe-oxidizing and S-oxidizing. We observed a large difference between the relative abundance of Fe-oxidizing bacteria and S-oxidizing bacteria based on 16S rRNA clone library and qPCR. Although the 16S rRNA clone library shows that the Fe-oxidizing bacteria of the order Ferritrophicales make up >60% of all clones in the clone library, S-oxidizing bacteria of the genus *Thiomonas* (order

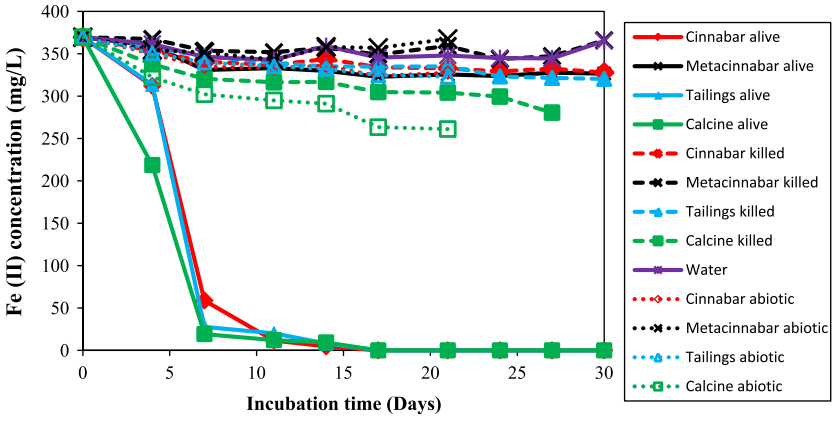

Fig. 4 Oxidation of Fe(II) during aerobic incubation of living cells. Error bars are smaller than the symbols, and the error is ± 0.1% (n = 3). The trend seen in the metacinnabar microcosm is identical to anaerobic incubation, killed controls, and abiotic controls. The experiment was conducted during August, 2008.

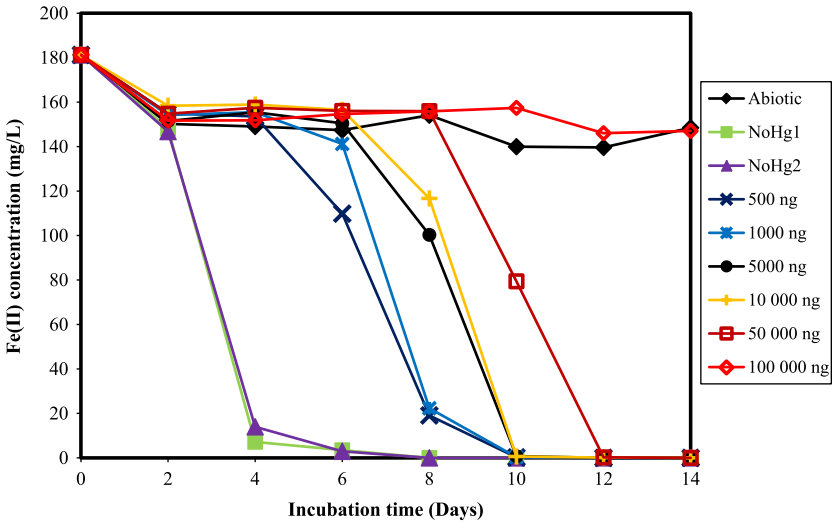

Fig. 5 Effect of added Hg to Fe(II) oxidation capability of the New Idria microbial community. Mercury was added to microcosms as $Hg(NO_3)_2$ and pH was held at pH = 4. Error bars are smaller than symbols, error is ± 0.1% (n = 3). Initial drop in Fe(II) concentration is assumed to be adsorption of Fe to the sides of the microcosm. Fe(II) accounts for 100% of the Fe at the beginning of the experiment. Experiment conducted during February, 2010.

Burkholderiales) account for only 14% of all clones in the top 1 cm of the AMD sediment. Because relative sequence abundance in clone libraries often does not reflect natural abundances, we also performed quantitative PCR analysis with *Thiomonas*-specific primers. qPCR revealed a relative abundance of this group of sulfur-oxidizing bacteria of about 55% of all bacteria in the top 1 cm of the AMD pond sediment. The relative underrepresentation of the *Thiomonas sp.* sequences in the clone library compared to the qPCR results can be explained by the use of primer sets with different specificity for both analyzes. Because NPOC of all microcosms remained relatively constant throughout the experiments, we hypothesize that the organic matter used by the community of heterotrophic microbes of the biofilm is derived from biomass of primary producers, such as the Fe(II) oxidizing bacteria in the biofilm. Due to the presence of S-oxidizing and Fe-oxidizing bacteria in the ecosystem with a high Hg tolerance, it is conceivable that both metabolic groups of micro-organisms might directly or indirectly be responsible for HgS dissolution within in AMD biofilm.

HgS dissolution

The dissolution of HgS within the New Idria AMD system occurs solely in the oxic zone. All anoxic microcosms showed a minor spike in Hg due to residual oxygen in the AMD water that was not purged prior to the start of the experiment (Fig. 3). Once the oxygen in the anoxic microcosms was consumed, the Hg concentrations either leveled off or dropped below detection. An increase in Hg released from abiotic and inactivated microcosms incubated in an oxic environment is most likely due to the organic matter contained in solution and mine waste materials (discussed later).

One explanation for the increased Hg concentration in microcosms is the presence of polysulfides, either present in solution or produced by the micro-organisms. Due to the low pH of the system and the lack of an increase in Hg in anoxic microcosms, polysulfides are not considered the driving factor for HgS dissolution in our experiments. Based on literature findings, polysulfides (and other reduced sulfide species) should not be stable in the New Idria AMD system because polysulfide formation and stability require neutral to basic pH as well as anoxic conditions (Paquette & Helz, 1995, 1997; Jay *et al.*, 2000). Although it is well known that biofilms can create microenvironments different than the surrounding environment, the fact that anoxic microcosms did not show any increase in Hg during the HgS dissolution experiments indicates that the AMD microbial community is not capable of producing an anoxic environment required for stable polysulfides or reduced sulfur species in the time frame of our experiments.

An explanation for why $HgS_{(s)}$ is degrading in the microcosms based solely on thermodynamics is not adequate. Both the cinnabar and metacinnabar polymorphs of HgS are quite insoluble, with solubility products of 10^{-54} and 10^{-52}, respectively (Faure, 1991; Krauskopf & Bird, 1995). Based on thermodynamic calculations of conditions within the microcosms, sulfide concentrations would need to drop to levels below 10^{-33} M in order to have HgS undersaturated at the New Idria site. A sulfide concentration of 10^{-33} M is unrealistic for any natural system and would result in supersaturation of the AMD solution with respect to HgS, making the abiotic release of Hg thermodynamically unfavorable. A study by Bura-Nakić *et al.* shows that even in oxic waters that are at or near O_2 saturation, concentrations of total reduced sulfur species are ~10^{-8} M (Bura-Nakic *et al.*, 2009). Several research groups

have published values for HgS stability in the presence of H_2S and its deprotonated forms (Paquette & Helz, 1995, 1997). Due to the low pH of the system, the dominant sulfide species will be H_2S. Calculated Hg concentrations, using background sulfide concentrations at the New Idria site, necessary for $HgS_{(s)}$ equilibrium would be ~10^{-12} M, which is significantly lower than the $10^{-8.5}$ M detected at the start of the experiment. Nearly, all of these chemical reactions require H_2S as a reactant, which would result in HgS becoming more stable as H_2S concentrations decrease. Because the initial experimental conditions were already supersaturated with regards to both cinnabar and metacinnabar, a purely abiotic thermodynamic explanation for the increase in Hg concentration in the microcosm is incorrect.

Another possible explanation for enhanced HgS dissolution at New Idria is that the S-oxidizing microbe is oxidizing H_2S in solution to sulfate, resulting in a drop in sulfide concentrations and leading to dissolution of HgS. This hypothesis suggests that every S-oxidizing bacterium in the environment would be capable of dissolving HgS. It has been assumed that S-oxidizing bacteria can slowly dissolve HgS, but there is little to no experimental evidence supporting this assumption (Wood, 1974; Madigan *et al.*, 2003). Research by Baldi and Olson using Hg-sensitive and Hg-tolerant *Thiobacillus ferrooxidans* strains with a mixture of pyrite and cinnabar showed that this Hg-tolerant bacterium was not capable of using cinnabar as the sole energy source (Baldi & Olson, 1987). Although experiments with the Hg-tolerant *Thiobacillus ferrooxidans* strain in a mixture of pyrite and cinnabar showed that Hg is released into solution as both Hg(II) and Hg^0, no Hg was released in experiments with cinnabar only. The release of Hg into solution was potentially attributed to back reactions of pyrite oxidation with HgS, since pyrite oxidation and Hg-release were found to be linked; however, no mechanism for this reaction was proposed (Baldi & Olson, 1987). Although not directly related to the work of Baldi and Olson, Wiatrowski *et al.* showed that magnetite can reduce Hg(II) to Hg^0 in anaerobic systems (Wiatrowski *et al.*, 2009).

The most likely hypothesis for HgS degradation in the New Idria AMD system, and potentially other inoperative Hg mine sites in California, is direct oxidation of the sulfide in the HgS crystals. Binding constants between Hg and S vary greatly depending on the oxidation state of S. As sulfur becomes more oxidized, the binding constants reduce greatly as seen in the following sequence: HS^- ($10^{37.71}$), $S_2O_3^{2-}$ ($10^{29.93}$), SO_3^{2-} ($10^{22.85}$), and SO_4^{2-} ($10^{1.34}$) (Smith & Martell, 2004). During oxidation of sulfide in HgS to sulfate, Hg should be released into solution from the mineral surface. The presence of sulfate at levels >2600 mg L^{-1} in the New Idria AMD system (Table 2) clearly demonstrates the oxidation of sulfur. In order to evaluate the role of S-oxidizing bacteria in HgS dissolution at the New Idria AMD site, we isolated a *Thiomonas sp.* strain from the tailings pond sediment. Because the obtained isolate had a Hg tolerance of >20 mg L^{-1} Hg, we evaluated the potential of this strain being responsible for the observed dissolution of HgS in the AMD system. However, when testing this *Thiomonas sp.* strain for HgS dissolution, we did not observe an increase of Hg(II) in the microcosms, suggesting that other members of the microbial community might be responsible for the observed biotic HgS dissolution. Because the media for the isolate experiments was created in the laboratory instead of using the water from the New Idria AMD system, it is highly probable that a constituent in the AMD water not included in the laboratory medium is necessary to facilitate *Thiomonas sp.* induced HgS dissolution. Another possibility for explaining HgS dissolution is that the process is indirectly coupled to microbial Fe-cycling. The experiment using the AMD microbial community and the settling pond water showed that Fe-cycling was important in those microcosms. The potential of Fe-cycling to help the micro-organisms with the dissolution of HgS is intriguing and requires additional work. One scenario for Fe-cycling impacting HgS dissolution is the creation of Fe(III) by microbial oxidation of Fe (II) in Fe-sulfides by back reaction with the sulfide in HgS, resulting in the oxidation of sulfide and concomitant dissolution of the HgS. Though this scenario has merit, currently there is no evidence for this occurring in the literature.

Regardless of the actual mechanism for HgS dissolution, it is evident that the New Idria microbial consortium has a profound influence on the solubility of HgS, both cinnabar and metacinnabar. Although the bioreactors are far from equilibrium, it is useful to compare the activity quotient for HgS dissolution in the AMD system with that of the idealized solubility constant for both HgS polymorphs. Activities for both sulfide and Hg^{2+} were calculated using both Geochemist's Workbench and Visual Minteq by using the sulfide concentration (metacinnabar alive, Day 3 sample, 0.1 μM), Hg_{tot} (metacinnabar alive, Day 3 sample, 18.7 μg L^{-1}), and the solution chemistry for the system (Table 2) (Bethke, 2002; Gustafsson, 2009). Using these calculated activities, a LogQ for HgS dissolution of −23.5 was calculated. Comparing activity quotient to the idealized HgS solubility for cinnabar and metacinnabar (LogK = −54 and −52, respectively), the New Idria biofilm is capable of increasing the solubility of HgS by 28.5–30.5 orders of magnitude for the bioreactor experiments.

In contrast with the experimental results described above, which showed that the bacterial consortium in the AMD system is mainly responsible for the greatly enhanced solubility of cinnabar and metacinnabar in the live oxic experiments, release of Hg from the abiotic and killed oxic controls is most likely due to organic matter from solution and the mine waste material used in the experiment. It is possible that outer membrane proteins not denatured

during the gamma irradiation were able to dissolve the HgS, but because abiotic and killed controls mirrored each other closely, the most likely cause of HgS dissolution in these microcosms is due to trace amounts of thiol groups associated with the organic matter (Fig. 3). Studies by numerous research groups have shown that organic matter rich in thiol groups such as humic and fulvic acids can actively dissolve HgS (Ravichandran *et al.*, 1998, 1999; Waples *et al.*, 2005). Because cell lysate, which is assumed to be the source of the organics in this system, have thiol containing functional groups, residual organic material in the system likely plays a minor role in HgS dissolution.

Effects of Hg on Fe-oxidation

Iron in the microcosms containing living biofilm material (oxic microcosms) was oxidized from Fe(II) to Fe(III) quickly in the cinnabar, tailings, and calcine reactor experiments (Fig. 4). In the metacinnabar microcosm, Fe (II) concentrations were similar to controls, suggesting inhibition of the Fe-oxidizing bacteria in the microcosm. The metacinnabar microcosms with living cells had an initial peak of Hg released into solution more than 24-fold greater than that of any other microcosm at day 8 of the HgS dissolution experiments (Fig. 2). The experiment investigating the effect of Hg concentrations on Fe(II) oxidation showed that concentrations close to that of the metacinnabar reactor caused a severe retardation in Fe-oxidation. As the HgS experiment progressed, the metacinnabar Hg_{tot} concentrations increased to levels above those required to inhibit Fe-oxidizing bacteria. The initial pulse of Hg into solution appears to have inactivated the Fe-oxidizing bacteria before they had a chance to grow and develop a higher Hg tolerance within the microcosm. The cinnabar, tailings, and calcine microcosms showed no such pulse in Hg concentration, which probably resulted

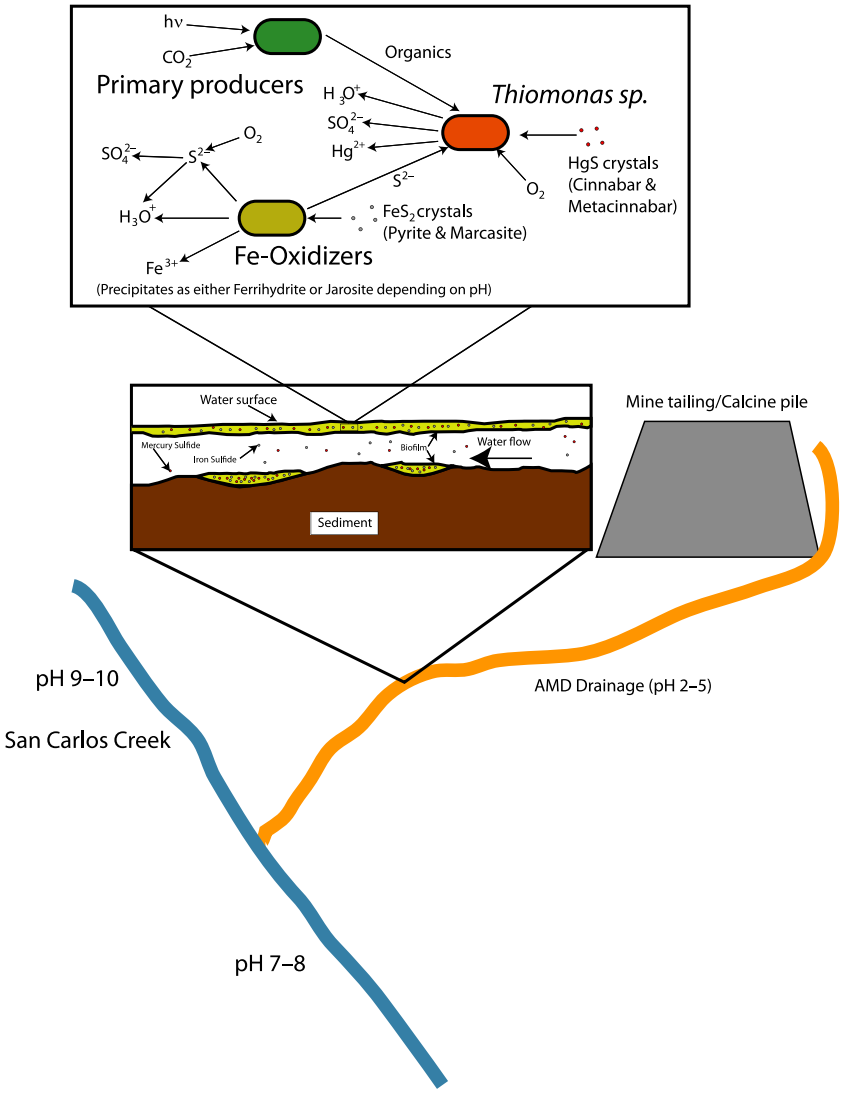

Fig. 6 Hypothetical cartoon of Fe and Hg cycling by the bacterial biofilm contained in the acid mine drainage system of the inoperative New Idria Hg mine. Mineal paricles are not drawn to scale. Most Fe- and Hg-sulfide particles released from the mine tailings and calcine pile are in the 10's to 100's of nm size.

in the Fe-oxidizing bacteria having sufficient time to adapt to the elevated Hg concentrations.

CONCLUSIONS

Although the primary microbial metabolism, based on the high concentrations of Fe(II) and Fe(III) and SO_4^{2-} at the inoperative New Idria Hg mine, is the breakdown of FeS_2 minerals (primarily marcasite), the breakdown of HgS is of greater importance to the ecosystems surrounding this and potentially other HgS-containing AMD systems in the California Coast Range. It has long been assumed that all S-oxidizing bacteria have the capability of dissolving HgS (Wood, 1974); however, this assumption has not been verified for systems with HgS as the sole mineral substrate. When compared with abiotic controls in which Hg concentrations drop below 1 ng L^{-1} throughout the experiments, this work clearly shows that the living microcosms have a tremendous impact on HgS stability. This study has also shown that the microbial community in the New Idria AMD system is capable of dissolving HgS and releasing Hg into solution as a soluble form and of enhancing the solubility of HgS by 28.5–30.5 orders of magnitude compared with the idealized solubility constants for both cinnabar and metacinnabar. Unlike experimental studies on the interaction of organic and reduced sulfur species with HgS in anoxic systems, the breakdown of HgS in aerobic systems is novel with wide-ranging implications for remediation of active and inactive Hg mine sites. Though aspects of HgS degradation in the New Idria AMD system are still unclear, a hypothetical model of the system is presented (Fig. 6). Whether the breakdown of HgS is through direct oxidation of the reduced sulfur on the HgS particle surface or is related to Fe-cycling is still unclear; however, the present study shows that micro-organisms can have a significant impact on the stability of HgS at inoperative Hg mines. This work provides clear evidence that even though HgS dissolution is highly thermodynamically unfavorable in most environmental systems, given the proper microbial community HgS can be broken down and become an even more potential hazard to downstream ecosystems than HgS crystals themselves. If HgS is dissolved and released into the downstream system in a form that is potentially highly bioavailable and easy to methylate, as this work shows for the New Idria AMD system, then a new pathway in the Hg cycle needs to be investigated in order to determine the best way to mitigate Hg-release from inoperative mine sites. Even though the dimensions of both the New Idria AMD system and microbial community are small and its Hg-release is thought to have a minor impact on the surrounding ecosystem, the results of this study serve as an indicator of potential Hg-release at other inoperative Hg mine sites in the California Coast Range and other sites worldwide that have developed an AMD system.

ACKNOWLEDGMENTS

We thank Ian Marshall of the Spormann research group and Phi Luong of the Brown research group for help with field sampling at the New Idria mine. We thank Petra Kühner for technical assistance with the qPCR experiments. Funding for this research came from the Stanford Environmental Molecular Science Institute through NSF Grant CHE-0431425 and from NSF Grant CBET-1235878.

REFERENCES

Aiken G, Haitzer M, Ryan JN, Nagy K (2003) Interactions between dissolved organic matter and mercury in the Florida Everglades. *Journal de Physique IV* **107**, 29–32.

Ashelford KE, Chuzhanova NA, Fry JC, Jones AJ, Weightman AJ (2006) New screening software shows that most recent large 16S rRNA gene clone libraries contain chimeras. *Applied and Environmental Microbiology* **72**, 5734–5741.

Baldi F, Olson GJ (1987) Effects of Cinnabar on pyrite oxidation by *Thiobacillus ferrooxidans* and Cinnabar mobilization by a mercury-resistant strain. *Applied and Environmental Microbiology* **53**, 772–776.

Baldi F, Filippelli M, Olson GJ (1989) Biotransformation of mercury by bacteria isolated from a river collecting cinnabar mine waters. *Microbial Ecology* **17**, 263–274.

Baldi F, Semplici F, Filippelli M (1991) Environmental applications of mercury resistant bacteria. *Water, Air, and Soil Pollution* **56**, 465–475.

Barkay T, Miller SM, Summers AO (2003) Bacterial mercury resistance from atoms to ecosystems. *FEMS Microbiology Reviews* **27**, 355–384.

Behrens S, Azizian MF, McMurdie PJ, Sabalowsky A, Dolan ME, Semprini L, Spormann AM (2008) Monitoring abundance and expression of "*Dehalococcoides*" species chloroethene-reductive dehalogenases in a tetrachloroethene-dechlorinating flow column. *Applied and Environmental Microbiology* **74**, 5695–5703.

Benoit JM, Gilmour CC, Mason RP, Heyes A (1999a) Sulfide controls on mercury speciation and bioavailablity to methylating bacteria in sediment pore waters. *Environmental Science & Technology* **33**, 951–957.

Benoit JM, Mason RP, Gilmour CC (1999b) Estimation of mercury-sulfide speciation in sediment pore waters using octanol-water partitioning and implications for availability to methylating bacteria. *Environmental Toxicology and Chemistry* **18**, 2138–2141.

Benoit JM, Mason RP, Gilmour CC, Aiken GR (2001) Constants for mercury binding by dissolved organic matter isolates from the Florida Everglades. *Geochimica et Cosmochimica Acta* **65**, 4445–4451.

Bethke CM (2002) The Geochemist's Workbench. Version 7.0, Aqueous Solutions LLC, Champaign, IL.

Bura-Nakic E, Helz GR, Ciglenecki I, Cosovic B (2009) Reduced sulfur species in a stratified seawater lake (Rogoznica Lake, Croatia); seasonal variations and argument for organic carriers of reactive sulfur. *Geochimica et Cosmochimica Acta* **73**, 3738–3751.

Cline JD (1969) Spectrophotometric determination of hydrogen sulfide in natural waters. *Limnology and Oceanography* **14**, 454–458.

Compeau GC, Bartha R (1985) Sulfate-reducing bacteria: principal methylators of mercury in anoxic estuarine sediment. *Applied and Environmental Microbiology* **50**, 498–502.

DeLong EF (1992) *Archaea* in coastal marine environments. *Proceedings of the National Academy of Sciences of the United States of America* **89**, 5685–5689.

Drexel RT, Haitzer M, Ryan JN, Aiken GR, Nagy KL (2002) Mercury(II) sorption to Two Florida Everglades peats: evidence for strong and weak binding and competition by dissolved organic matter released from the peat. *Environmental Science & Technology* **36**, 4058–4064.

Fagerstrom T, Jernelov A (1971) Formation of methyl mercury from pure mercury sulphide in aerobic organic sediment. *Water Research* **5**, 121–122.

Faure G (1991) *Principles and Applications of Geochemistry*. Prentice Hall, Upper Saddle River.

Fleming EJ, Mack EE, Green PG, Nelson DC (2006) Mercury methylation from unexpected sources: molybdate-inhibited freshwater sediments and an iron-reducing bacterium. *Applied and Environmental Microbiology* **72**, 457–464.

Gustafsson JP (2009) Visual MINTEQ. Version 2.61, Stockholm, Sweden.

Haitzer M, Aiken GR, Ryan JN (2003) Binding of Mercury(II) to aquatic humic substances: influence of pH and source of humic substances. *Environmental Science & Technology* **37**, 2436–2441.

Hayashi K, Kawai S, Ohno T, Maki Y (1977) Photomethylation of inorganic mercury by aliphatic α-Amino-acids. *Journal of the Chemical Society-Chemical Communications*, 158–159.

Huber T, Faulkner G, Hugenholtz P (2004) Bellerophon: a program to detect chimeric sequences in multiple sequence alignments. *Bioinformatics* **20**, 2317–2319.

Jay JA, Morel FMM, Hemond HF (2000) Mercury speciation in the presence of polysulfides. *Environmental Science & Technology* **34**, 2196–2200.

Kalyaeva ES, Kholodii GY, Bass IA, Gorlenko ZM, Yurieva OV, Nikiforov VG (2001) Tn*5037*, a Tn*21*-like mercury resistance transposon from *Thiobacillus ferrooxidans*. *Russian Journal of Genetics* **37**, 972–975.

Kim CS, Brown GE Jr, Rytuba JJ (2000) Characterization and speciation of mercury-bearing mine wastes using x-ray absorption spectroscopy. *The Science of the Total Environment* **261**, 157–168.

Kim CS, Rytuba JJ, Brown GE Jr (2004) Geological and anthropogenic factors influencing mercury speciation in mine wastes: an EXAFS spectroscopy study. *Applied Geochemistry* **19**, 379–393.

King JK, Kostka JE, Frischer ME, Saunders FM (2000) Sulfate-reducing bacteria methylate mercury at variable rates in pure culture and in marine sediments. *Applied and Environmental Microbiology* **66**, 2430–2437.

Krauskopf KB, Bird DK (1995) *Introduction To Geochemistry*. WCB/McGraw-Hill, Boston, MA.

Lane D, Pace B, Olsen G, Stahl D, Sogin M, Pace N (1985) Rapid determination of 16S ribosomal RNA sequences for phylogenetic analyses. *Proceedings of the National Academy of Sciences of the United States of America* **82**, 6955–6959.

Lee ZM-P, Bussema C III, Schmidt TM (2009) rrnDB: documenting the number of rRNA and tRNA genes in bacteria and archaea. *Nucleic Acids Research* **37**(suppl 1), D489–D493.

Linn RK (1968) New Idria Mining District. In *Ore Deposits of the United States, 1933–1967*, vol. **2** (ed. Ridge JD). The American Institute of Mining, Metallurgical, and Peroleum Engineers, Inc., New York, pp. 1623–1649.

Lowry GV, Shaw S, Kim CS, Rytuba JJ, Brown GE Jr (2004) Macroscopic and microscopic observations of particle-facilitated mercury transport from New Idria and sulphur bank mercury mine tailings. *Environmental Science & Technology* **38**, 5101–5111.

Ludwig W, Strunk O, Westram R, Richter L, Meier H, Yadhukumar, Buchner A, Lai T, Steppi S, Jobb G, Forster W, Brettske I, Gerber S, Ginhart AW, Gross O, Grumann S, Hermann S, Jost R, Konig A, Liss T, Lussmann R, May M, Nonhoff B, Reichel B, Strehlow R, Stamatakis A, Stuckmann N, Vilbig A, Lenke M, Ludwig T, Bode A, Schleifer K-H (2004) ARB: a software environment for sequence data. *Nucleic Acids Research* **32**, 1363–1371.

Madigan MT, Martinko JM, Parker J (2003) *Brock Biology of Microorganisms*. Prentice Hall, Upper Saddle River.

Massana R, Murray AE, Preston CM, Delong EF (1997) Vertical distribution and phylogenetic characterization of marine planktonic *Archaea* in the Santa Barbara channel. *Applied and Environmental Microbiology* **63**, 50–56.

Materials Data Inc. (2002) *Jade XRD Pattern Processing Ver. 6.5*, Materials Data Inc., Livermore, CA.

Mindlin S, Kholodii G, Gorlenko Z, Minakhina S, Minakhin L, Kalyaeva E, Kopteva A, Petrova M, Yurieva O, Nikiforov V (2001) Mercury resistance transposons of gram-negative environmental bacteria and their classification. *Research in Microbiology* **152**, 811–822.

Muyzer G, de Waal EC, Uitterlinden AG (1993) Profiling of complex microbial populations by denaturing gradient gel electrophoresis analysis of polymerase chain reaction-amplified genes coding for 16S rRNA. *Applied and Environmental Microbiology* **59**, 695–700.

Paquette K, Helz G (1995) Solubility of Cinnabar (Red HgS) and implications for mercury speciation in sulfidic waters. *Water, Air, and Soil Pollution* **80**, 1053–1056.

Paquette KE, Helz GR (1997) Inorganic speciation of mercury in sulfidic waters: the importance of zero-valent sulfur. *Environmental Science & Technology* **31**, 2148–2453.

Pruesse E, Quast C, Knittel K, Fuchs BM, Ludwig W, Peplies J, Glockner FO (2007) SILVA: a comprehensive online resource for quality checked and aligned ribosomal RNA sequence data compatible with ARB. *Nucleic Acids Research* **35**, 7188–7196.

Ravichandran M, Aiken GR, Reddy MM, Ryan JN (1998) Enhanced dissolution of cinnabar (mercuric sulfide) by dissolved organic matter isolated from the Florida Everglades. *Environmental Science & Technology* **32**, 3305–3311.

Ravichandran M, Aiken GR, Ryan JN, Reddy MM (1999) Inhibition of precipitation and aggregation of metacinnabar (mercuric sulfide) by dissolved organic matter isolated from the Florida Everglades. *Environmental Science & Technology* **33**, 1418–1423.

Reddy MM, Aiken GR (2001) Fulvic acid-sulfide competition for mercury ion binding in the Florida Everglades. *Water, Air, and Soil Pollution* **132**, 89–104.

Rytuba JJ (2003) Mercury from mineral deposits and potential environmental impact. *Environmental Geology* **43**, 326–338.

Smith RM, Martell AE (2004) *NIST Critically Selected Stability Constants of Metal Complexes Database*. NIST Standard Reference Database. National Institute of Standards and Technology, Washington D.C., Version 8.0.

Stookey LL (1970) Ferrozine-A new spectrophotmetric reagent for iron. *Analytical Chemistry* **42**, 779–781.

Ullrich SM, Tanton TW, Abdrashitova SA (2001) Mercury in the aquatic environment: a review of factors affecting methylation. *Critical Reviews in Environmental Science and Technology* **31**, 241–293.

U.S. EPA (2002) *Method 1631, Revision E: Mercury in Water by Oxidation, Purge and Trap, and Cold Vapor Atomic Fluorescence Spectrometry*. U. S. Environmental Protection Agency, Washington D.C.

Waples JS, Nagy KL, Aiken GR, Ryan JN (2005) Dissolution of Cinnabar (HgS) in the presence of natural organic matter. *Geochimica et Cosmochimica Acta* **69**, 1575–1588.

Weishaar JL, Aiken GR, Bergamashi BA, Fram MS, Fujii R, Mopper K (2003) Evaluation of specific ultraviolet absorbance as an indicator of the chemical composition and reactivity of dissolved organic carbon. *Environmental Science & Technology* **37**, 4702–4708.

Wiatrowski HA, Das S, Kukkadapu R, Ilton ES, Barkay T, Yee N (2009) Reduction of Hg(II) to Hg(0) by magnetite. *Environmental Science & Technology* **43**, 5307–5313.

Wood JM (1974) Biological cycles for toxic elements in the environment. *Science* **183**, 1049–1052.

Zhou J, Bruns MA, Tiedje JM (1996) DNA recovery from soils of diverse composition. *Applied and Environmental Microbiology* **62**, 316–322.